Journal of Cleaner Production 245 (2020) 118702

Contents lists available at ScienceDirect

Journal of Cleaner Production

journal homepage: www.elsevier.com/locate/jclepro

Deep learning-driven particle swarm optimisation for additive manufacturing energy optimisation

Jian Qin [a], Ying Liu [a, *], Roger Grosvenor [a], Franck Lacan [a], Zhigang Jiang [b]

[a] Institute of Mechanical and Manufacturing Engineering, School of Engineering, Cardiff University, Cardiff, CF24 3AA, UK
[b] Hubei Key Laboratory of Mechanical Transmission and Manufacturing Engineering, Wuhan University of Science & Technology, Wuhan, 430081, China

ARTICLE INFO

Article history:
Received 31 March 2019
Received in revised form
17 August 2019
Accepted 2 October 2019
Available online 7 October 2019

Handling editor: Tomas B. Ramos

Keywords:
Additive manufacturing
Energy consumption modelling
Prediction and optimisation
Deep learning
Particle swarm optimisation

ABSTRACT

The additive manufacturing (AM) process is characterised as a high energy-consuming process, which has a significant impact on the environment and sustainability. The topic of AM energy consumption modelling, prediction, and optimisation has then become a research focus in both industry and academia. This issue involves many relevant features, such as material condition, process operation, part and process design, working environment, and so on. While existing studies reveal that AM energy consumption modelling largely depends on the design-relevant features in practice, it has not been given sufficient attention. Therefore, in this study, design-relevant features are firstly examined with respect to energy modelling. These features are typically determined by part designers and process operators before production. The AM energy consumption knowledge, hidden in the design-relevant features, is exploited for prediction modelling through a design-relevant data analytics approach. Based on the new modelling approach, a novel deep learning-driven particle swarm optimisation (DLD-PSO) method is proposed to optimise the energy utility. Deep learning is introduced to address several issues, in terms of increasing the search speed and enhancing the global best of PSO. Finally, using the design-relevant data collected from a real-world AM system in production, a case study is presented to validate the proposed modelling approach, and the results reveal its merits. Meanwhile, optimisation has also been carried out to guide part designers and process operators to revise their designs and decisions in order to reduce the energy consumption of the designated AM system under study.

1. Introduction

AM has developed as an essential manufacturing system in Industry 4.0 (Eyers and Potter, 2017; Huang et al., 2013). Different from the AM production of prototypes 30 years ago, current AM applications focus on producing end-use parts. According to an AM financial report (Wohlers, 2016), the market of AM production will be worth over 20 billion USD by 2020. Because of the potential market's size, AM is known as one of the most popular manufacturing processes, which makes AM sustainability become a crucial research topic (Niaki et al., 2019). Under this large and interesting topic, many issues have never failed to attracted researchers' attention, such as material selection and consumption, particle emission, and energy consumption (Junk and Coté, 2013). Among these interesting topics, reducing energy consumption is one of the most signification drivers for environmental improvement, and cost-saving of AM processes (Verhoef et al., 2018; Jiang et al., 2019). AM energy consumption is a comprehensive issue which involves multiple manufacturing phases, pre-process, building process, and post-process (Yosofi et al., 2019). Especially in the building process, it is affected by the various factors including material condition, process operation, part and process design, and working environment, (Baumers et al., 2011a; Qin et al., 2017).

Since AM's high design freedom for producing end-use parts, AM processes provide part designers with a valuable opportunity to produce a wide range of parts (Thompson et al., 2016). However, the high design freedom of production also results in the AM process more complicated, in terms of complex mechanical structures and unique design features. Furthermore, in some multiple-part production processes, such as selective laser sintering (SLS) and selective laser melting (SLM) (Gibson et al., 2010), a single AM production process can build several different parts at the same time. In these processes, the orientations and locations of the parts are determined by process operators, which is noted as an AM

* Corresponding author.
E-mail address: liuy81@cardiff.ac.uk (Y. Liu).

https://doi.org/10.1016/j.jclepro.2019.118702
0959-6526/

process planning issue (Zhang et al., 2014). With the high design freedom in part production and the various processing plans in each AM process, AM systems are able to create countless possibilities for diverse part production, offering part designers and process operators a variety of options in part and process design (Peng et al., 2018).

In order to help part designers and process operators to understand AM process design, design for additive manufacturing (DfAM) was proposed. The term DfAM is derived from design for manufacturing and assembly (DfMA) (Thompson et al., 2016). Similar to DfMA, DfAM includes numerous design-relevant aspects, such as material design, part geometry design, and process planning, each of which involves many design-relevant features (Gibson et al., 2010). These features also play into the factors, that impact AM energy consumption, which are decided before starting the producing process by part designers and process operators (Qin et al., 2018; Ding et al., 2018). Modelling the design-relevant data of AM systems to predict energy consumption, and then reducing it by optimising the designs and decisions of part designers and process operators have become a crucial research topic for improving AM systems (Baumers et al., 2011b; Panda et al., 2016; Watson and Taminger, 2018).

Among the various optimisation algorithms, particle swarm optimisation (PSO) is a powerful algorithm that is able to solve nonlinear multi-objective problems so as to help relevant professionals for decision-making (Bai, 2010; Chen and Huang, 2017; Moradi and Abedini, 2012). Generally, the searching speed of the particles is adjusted by equal parameters in conventional PSOs (Kennedy, 2011; Kim and Son, 2012). These parameters are defined by constant inertia weight and cognitive factors (Shi, 2001). However, since each relevant feature may have various types of relationship with the optimised target, it is necessary to introduce variable particle searching speed based on the correlations between each feature and the optimised target. Deep learning, as an advanced machine learning technique, has shown its merits in prediction modelling based on high-dimensional and large-scale data (LeCun et al., 2015a). It has also shown its sensitivity to correlate the relevant features, which is represented by neuron activity (Kim et al., 2016). If this functional characteristic can be adapted to drive PSO, each feature will use a different searching speed in order to achieve the optimised value. If this is possible, it not only improves the convergence speed but also enhances the global best of PSO.

This paper proposes a prediction approach based on deep learning techniques with a focus to explore whether design-relevant data has a significant impact on AM energy consumption. Additionally, a novel deep learning-driven PSO (DLD-PSO) algorithm is proposed to reduce AM energy consumption. The main factors in DLD-PSO, such as constant inertia weight and cognitive factors, are driven by the deep learning model. The rest of the paper is structured as follows. Section 2 reviews studies on DfAM sustainability and AM energy consumption and discusses PSO methods which improve manufacturing processes. In Section 3, an energy consumption modelling approach and the DLD-PSO algorithm which use design-relevant data are proposed. This data was collected from the decisions of two groups of professionals, part designers, and process operators. Section 4 presents a case study on prediction and reduction of the energy consumption of an SLS system. Results are compared and discussed to reflect the performance of the proposed approach in Section 5. Section 6 concludes.

2. Literature review

2.1. Design for additive manufacturing (DfAM)

AM provides designers with unique and far-reaching freedom to optimise their designs, which makes the design of part production and processes more sustainable (Gebisa and Lemu, 2017). The parts produced by AM processes are also generally more complex than conventional manufacturing parts, in terms of geometry and internal structure. Current studies on DfMA typically focus on the standard geometric parts that are produced by conventional manufacturing systems. It makes DfMA methods no longer suitable for use in AM design (Li et al., 2019). Furthermore, there exists an urgent need to provide AM design professionals with a greater range of design and analysis tools for complex part structures and AM processes, DfAM has been proposed as a way to address such design problems in AM processes (Tang and Zhao, 2016).

Ma et al. (2018) proposed a framework that integrates part lifecycle sustainability with AM product design. In this framework, the AM part lifecycle was described in detail including the part design, production process design, cost and usage control, and end-of-life handling stages. The part design and process planning were the most critical aspects of their framework and was highlighted throughout it. In the framework, input features included energy, material support, equipment, and logistics. Process costs, environmental impacts, and potential human toxicity were modelled as the output values. To validate the framework, the authors presented a case study targeted at a gear. This study handled each factor of its framework independently, but the described stages—from part design to end-of-life handling—interact, meaning that every stage affects the others. Furthermore, it only produced a lifecycle analysis (LCA) results without any optimisation.

Thompson et al. (2016) reviewed over 300 research articles to summarise the research status, trends, challenges, and opportunities of and for DfAM. The authors of this paper claimed that DfAM was substantially different from conventional manufacturing assembly design in many aspects, such as knowledge, tools, rules, processes, and methodologies. They believed that AM processes require a new design framework because they involve various irregular factors, such as production time, cost, batch size, and so on, in contrast to conventional manufacturing processes. Additionally, the study reviewed a significant number of related works, which covered such topics as part geometry design, process design, and AM material design. Notably, the importance of DfAM was emphasised in cases that examined multiple customised parts produced by AM processes. On top of understanding functional optimisation, understanding sustainable optimisation is another significant objective of reviewing these DfAM studies, and this was highlighted throughout the paper. Tang and Zhao (2016) published a survey of the sustainability of DfAM. This paper focused on LCA and environmental impacts motivating product designers to optimise AM processes designs. The authors of this survey mentioned that the existing design methods for the AM process primarily focused on fine-tuning product functional performance including size, shape, and topology optimisation.

Gardan and Schneider (2015) introduced a design optimisation method for improving the part structure of the SLS process that discovered the knowledge of manufacturing limitation and situation from the SLS process. Further, a unique design structure that can clean unused powders augmented to this method's optimised results. However, these optimisations are considered to be unable to match the fabrication capabilities of AM processes; the researchers must examine the process's design methods in more detail (Tang and Zhao, 2016). Moreover, Gebisa and Lemu (2017) pointed out that sustainability is an essential component of DfAM and discussed how current AM processes are not sufficiently energy-efficient, as general manufacturing design principles are not suitable for use with them.

Based on this understanding of DfAM, Tang et al. (2016b) proposed a framework that integrated design elements in LCA

assessment with the AM process. This framework used an LCA model to assess the environmental impacts of the AM process, and design-relevant data was input into the framework. Moreover, they proposed a design for optimising energy consumption and material used according to this method. The paper also presented a case study validating the framework's performance, using an aircraft engine bracket as the target product. Following the framework process, an optimised engine bracket design was created for production through AM remained the primary objective and kept the safety factors. The produced design required approximately 47% less material than did the original design; this figure was also lower than those of the optimised designs of conventional manufacturing processes, like the computer numerical control (CNC) process, by 22%. To produce new parts, more than half of the CO_2 equivalents were either for AM or conventional processes. However, this new design only facilitated a production energy consumption approximately 2% lower than that of the original design through both the AM process and the conventional process. It is apparent that reducing energy consumption was more difficult than was optimising other LCA assessment indicators. The framework was considered as one of the fundamental architectures for AM process designers who seek to optimise their designs to protect the environment (Tang et al., 2016b).

According to the above research on DfAM, it is widely viewed as one of the most necessary aspects of AM systems, especially for sustainability analysis. Additionally, the current research of DfAM tends to integrate LCA assessment for design optimisation, and optimisations and seeks to reduce material and energy usage in production to minimise environmental impacts and production costs. In Section 2.2, AM energy consumption analysis research is reviewed, and design is emphasised as the main factor impacting it.

2.2. Design-relevant impacts on AM energy consumption

AM energy consumption analysis, an essential aspect of sustainability optimisation, has never failed to attract researchers' attention. Comparing to some other conventional manufacturing processes, such as bulk-forming, the energy consumption of the AM process is higher (Yoon et al., 2014). Different AM technologies have various levels of energy consumption, due to the different working principles. The energy consumption under a particular AM technology varies in a wide range. The energy consumption is affected by many factors of AM processes, including process parameter settings, working environment, material conditions, and product design (Qin et al., 2017).

However, design-related impacts are often overlooked due to their complexity. Zhang et al. (2018a) believed that a bio-inspired part design could improve sustainability through functionality improvements, the reduction of material usage and energy consumption, and the introduction of smaller environmental impacts. They applied this idea to the part design stage in the AM process and proposed a conceptual model for redesigning areas of the AM process. This model integrated DfAM principles with bio-inspired design aspects, such as material features, production process parameters, and product functionality. A case study was conducted which compared three different part filling structures (diamond, honeycomb, and bone) using an SLS process. The bone structure was considered the bio-inspired structure in this study, and many factors relating to the structures, such as their physical properties, basic stress analysis results, energy consumption rates, and other LCA assessments, were compared. Notably, the energy consumption of the bone structure was found to be lower than that of the honeycomb structure by 8% and that of the diamond structure by 12%. The bio-inspired geometrical design highlighted in this paper provided a solution for the structural design of the AM process which reduced energy consumption and maintains product functionality.

Aside from parts' filling structures, other design-relevant factors also draw researchers' attention. Panda et al. (2016) pointed out that slice thickness and part orientation were two significant factors in determining AM energy consumption. An optimised framework based on genetic programming was proposed to develop the relationship between energy consumption, slice thickness, and part orientation. In their experiment, slice thickness varied between 0.02 mm and 0.10 mm in intervals of 0.02 mm and part orientation varied between 0° and 45° in 5° intervals. Other process parameter settings were kept the same. Based on this approach, energy consumption can be predicted with an error rate of approximately 3.45%. Based on the idea that slice thickness and part orientation were two important aspects of AM energy consumption, Paul and Anand (2012) also conducted several experiments on part orientation. In these experiments, three geometric primitives (a cube, a cylinder, and a functional part) were built in three slice thicknesses (0.03 mm, 0.05 mm, and 0.10 mm) and three part-orientations (0°, 30°, and 45°). The energy consumption of the production process was then monitored. For each geometric primitive, energy consumption decreased as slice thickness increased and orientation degree decreased. However, it is difficult to compare the amount of energy consumed in the production of these three geometric primitives because these experiments monitored total energy consumption rather than the unit energy consumption of each process. According to the above studies, filling structure, slice thickness, and part orientation impact AM energy consumption. However, only a single part was built in each AM production experiment, which happens rarely in current AM production processes (particularly SLS and SLM).

Baumers et al. (2011b) claimed that differences in energy consumption were revealed between processes in which a single part was built and processes in which multiple parts were built. In their study, 6 a.m. systems, including SLS, SLM, electron beam melting (EBM), and fused deposition modelling (FDM), were tested and compared; each system produced both a single part and multiple parts within a single production process. On average, building multiple parts costed approximately 25% less energy than did the production of single parts, and the SLS system was found to use 97% less energy than the other systems examined in this study. However, it is difficult to draw a conclusion on the energy consumption behaviours of these systems based on these experiments alone. Further, each experiment used the part design that was based on the single-part production process to generate a multiple-part production process design. In an AM process, various part designs are combined and built together to produce a suitable process design. Moreover, the chosen process plan varied in terms of orientation and part positioning for each AM technology that was used; this was not addressed in the paper. Therefore, due to the complex process and various impacts, it is necessary to apply real data rather than experimental data to analyse and model AM energy consumption.

In our previous work (Qin et al., 2018), an AM energy consumption modelling approach was proposed, in which multi-source data, such as working environmental data, process operation data, design-relevant data, and material condition data, was sensed and collected. The resulting dataset contained 12 variables, including the average height of a single part, the total height of the build, the filling degree, and the number of parts built in each individual process. These variables were extracted from both the part design and process planning stages. The prediction-based model integrated deep learning and clustering techniques, which fused the multiple sources and level data together. The results demonstrated the merit of the proposed approach in comparison to that of

the predictive modelling method by applying single-source input data. Although the study built an accurate AM energy consumption prediction model, the input data were collected both before and during the process. The prediction model was also hard to use to reduce AM energy consumption. To optimise energy consumption, the model should be built before the production process begins so that it is necessary to sense and collect the input data before this point.

Previous research on the design-relevant impacts of AM energy consumption shows that AM design-relevant features have been widely used to construct prediction models. However, previous studies tended to conduct experiments based on design-relevant data or integrate it with other types of data from AM processes. A need exists to predict AM energy consumption based only on design-relevant features and to optimise such features to reduce energy consumption. In Section 2.3, PSO, one of the most popular optimisation methods in manufacturing processes, is reviewed.

2.3. PSO for manufacturing process optimisation

PSO is one of the most famous evolutionary algorithms used to solve continuous, non-linear, multi-objective optimisation problems (Kuo and Lin, 2010; Tang et al., 2016a). Theoretically, the typical PSO method works by sending out a swarm of particles to search for the best result according to the required limitations; each particle represents a feasible solution to the given problem (Zou et al., 2019). It has been commonly used to solve manufacturing process optimisation problems (Yusup et al., 2012).

Bensingh et al. (2019) introduced a hybrid approach that combines artificial neural networks (ANN) and PSO to optimise the injection modelling process parameters. In their study, the injection modelling process produced a bi-aspheric lens. The quality of the lens and its upper process capability was the model's optimisation validation metrics, and it was represented through the three main measures of each side of the bi-aspheric lens: radius of curvature, surface roughness, and waviness. In this study, seven parameters were optimised to improve the quality of products. An ANN-based model was used to predict lens quality based on the injection modelling process parameters. Training and testing data were collected from the 44 experiments conducted over the course of the study. Based on the ANN prediction model, PSO was applied to optimise the parameters of the NN structure, including its number of neural layers, to improve the model's performance. The optimised results were compared to the GA-optimised ANN, and the proposed approach was found to return fewer errors and present a faster convergence speed than traditional PSO. The optimisation provided by PSO was proven to be better than that of GA. However, one of the six main outputs, the waviness of the shallow profile, was predicted with a substantial error larger than the mean error of the original values.

Ye et al. (2018) proposed a PSO-based method for optimising AM processes which features stochastic finite element analysis (SFEA). SFEA was used to model the output value which was the residual stress in thin-walled parts. PSO was used to find the maximum value of the target within the limitations. The proposed method began by extracting the process parameters, such as layer thickness, melting temperature, scanning speed, and hotbed temperature flux, from the process. Also, the CAD part design model was considered a potential input variable for the SFEA model. The results of their case study were reasonable, and their research involved collecting part design data to characterise one of the essential process factors. This emphasises the necessity of carrying out further DfAM research.

Raju et al. (2018) proposed a hybrid PSO method integrated with bacterial foraging optimisation (BFO) to solve mechanical and surface quality problems of AM processes, such as those introduced by varying hardness, flexural modulus, tensile strength, and surface roughness. Four parameters were considered as the input into the simulation model: layer thickness, support material, model interior, and orientation. The model was built through multiple linear regression. Two types of the designed parts were printed to model data collection, and 18 samples were produced for each. Three parameter setting combinations were used to uncover the best solution to each mechanical and surface quality problem. The PSO−BFO algorithm was then used to find the best parameter settings. This study exemplified the advantages PSO can offer AM parameter optimisation and how it can be easily integrated with other algorithms for exceptional results. However, the authors selected the constant inertia weight and cognitive factors for the proposed PSO−BFO model without providing an explanation of either choice.

Janahiraman et al. (2018) introduced a hybrid method that integrates extreme learning machine with PSO to optimise CNC processing and product surface roughness. Two stages were identified as essential in their paper: modelling and optimisation. PSO was used for optimisation. Three inputs were used for modelling: cutting speed, feed rate, and cut depth. A difference of 24% was found to exist between the predictive results returned by this model and the real-world results. Additionally, it identified optimal parameter settings. Task scheduling presents another problem that is often solved by PSO methods. Zhang et al. (2018b) published an article addressing the digital array radar (DAR) task scheduling problem, which was defined as an N−P problem and was, therefore, difficult to solve using only the meta-heuristic method. In this study, an integer programming optimisation model was built to establish the DAR task structure and was formed of multiple aspects. In addition, a hybrid PSO was proposed for improving efficiency in task scheduling schemes. This study adopted chaotic sequences and Shannon entropy equation to improve the quality of the initialized points and the convergence speed. When compared to three other scheduling optimisation methods (the online interleaving algorithm, GA−PSO, and the HPF algorithm), the proposed optimisation method obtained the highest successful scheduling ratio from the same number of targets. PSO improved when the initialized point and convergence speed coefficients were changed. The study was championed by many other researchers as one of the most important studies for PSO improvement. For example, Kennedy (2011) suggested setting the convergence coefficients as 2.05 and the initial coefficient as 0.7298 to improve the convergence speed of PSO.

Accordingly, the design-relevant features of AM processes have drawn much attention, especially in terms of the sustainability of DfAM, as these features have crucial impacts on AM energy consumption. However, current research has not focused sufficient attention on AM energy consumption analysis based on design-relevant features. It is necessary to build an accurate energy consumption model by using design-relevant data. Energy consumption can then be reduced by optimising the model's design. PSO is a popular optimisation method for solving this problem. In Section 3, a deep learning-based energy consumption model is proposed, and an adaptive PSO method for reducing the energy consumption of the deep learning model is then introduced.

3. Methodology

In this work, the AM energy consumption is predicted by only using design-relevant data as input. The modelling process is displayed in Section 3.1. Then, deep learning-based PSO is proposed to optimise design-relevant features for reducing energy consumption. Before introducing the details of the methodology, the list of nomenclature is displayed in Table 1.

3.1. AM energy consumption modelling based on the design-relevant data

In order to predict energy consumption for AM systems based on the design-relevant data, a deep learning-based approach is proposed in this study. The proposed AM energy consumption modelling process is shown in Fig. 1.

Firstly, the design-relevant data (D_i) is used for predicting the process data. The process data includes various datasets, such as working environment dataset, process operation dataset (parameter setting data), and material condition dataset. Each of these datasets can also involve different data attribute. For example, the process operation dataset consists of the parameter settings of laser power, scan space, scan speed, and scan angle. It is noticed that a different system may involve different attributes. More details of multi-source data analytics for AM energy consumption has been introduced and discussed in our previous work (Qin et al., 2018). The first deep learning-based prediction model $f_p(*)$ is built using the design-relevant data and historical process data (L_j), shown as follows:

$$L_j = f_p(D_i) \tag{1}$$

$$E_U = f_m(D_i, L_j) \tag{2}$$

Due to these two datasets are classified into two levelled datasets (Qin et al., 2018), the merged neural network $f_m(*)$ is used for integrating the predicted process data and design-relevant data and predicting the unit energy consumption (E_U), which is donated as equation (2). The details of the merged neural network ($f_m(*)$) are explained in the previous paper (Qin et al., 2018). This energy consumption modelling is based on deep learning techniques, and two neural networks are applied in the approach. The design-relevant data is used as the primary input data. Based on this prediction modelling, a deep learning-driven PSO is proposed to reduce the AM energy consumption by optimising the design-relevant features.

3.2. DLD-PSO for AM energy optimisation

To initialize the particles, the restriction of each design-relevant feature is necessary to identify. Due to the high-relevance between these features and design, it is essential to identify the sources of the design. Generally, the design features of the AM process are defined by two group people, part designers and process operators (Chergui et al., 2018). The design-relevant data is then categorised as two datasets, part-design dataset, and process-planning dataset, which is donated as:

$$D_i = [PD_g, PP_h] \tag{3}$$

where PD represents the part-design dataset which the number of g features, PP is the process-planning dataset which the number of h features.

The purpose of optimising the AM energy consumption is to the minimum energy usage of the AM process. The objective functions are defined as:

$$Min\ [f_m(D_i, L_j)] \tag{4}$$

$$s.t.: PD^m_{min} \le PD_m \le PD^m_{max} \tag{5}$$

$$PP^n_{min} \le PP_n \le PP^n_{max} \tag{6}$$

where the PD^m_{min} and PD^m_{max} are the minimum and maximum of the part-design dataset that is determined by part designers. The PP^n_{min} and PP^n_{max} are the restrictions of the process-planning dataset that is determined by process operators.

The DLD-PSO is proposed to solve the AM energy optimisation problem in this study. The optimisation process is shown in Fig. 2. Firstly, the particle restriction is initialized by part designers and process operators respectively. In the restriction, the initial particles are generated. The fitness values are calculated by the function (2). Then, the fitness value of each particle is compared to find the best values, lowest energy consumption, which is defined as the personal best (p_{best}). Once the new personal best is targeted, the global best particle (g_{best}) is also found from the best particle's personal best. After that, new particles in each interval are expressed by the following equation:

Table 1
This table shows the list of nomenclature which is used in Methodology.

Symbol	Property	Symbol	Property
$\boldsymbol{D_i}$	Design-relevant data	$\boldsymbol{p_{best}(t)}$	Personal best particle
$\boldsymbol{f_p(*)}$	ANN based prediction model	$\boldsymbol{C_2}$	Cognitive factor 2
$\boldsymbol{L_j}$	Historical process data	$\boldsymbol{g_{best}(t)}$	Global best particle
$\boldsymbol{E_U}$	Unit energy consumption	$\boldsymbol{w^i_d}$	Weights of all neurons
$\boldsymbol{f_m(*)}$	Merged neural network	$\boldsymbol{K}$	Total number of neurons in the first layer
$\boldsymbol{i}$	The i^{th} build dataset	$\boldsymbol{k}$	The k^{th} neuron
$\boldsymbol{PD_g}$	Part-design data	$\boldsymbol{e}$	Total number of design-relevant features
$\boldsymbol{PP_h}$	Process-planning data	$\boldsymbol{E_T}$	Total energy consumption of each build
$\boldsymbol{g}$	Number of part-design features	$\boldsymbol{M_T}$	Producing parts total weight
$\boldsymbol{h}$	Number of process-planning features	$\boldsymbol{E_e}$	Energy consumption of a consumer
$\boldsymbol{PD^g_{min}}$	Minimum restriction of part-design data	$\boldsymbol{T}$	Production time of one build
$\boldsymbol{PD^g_{max}}$	Maximum restriction of part-design data	$\boldsymbol{e_{RMSE}}$	The value of root-mean-square-error
$\boldsymbol{PP^h_{min}}$	Minimum restriction of process-planning data	$\boldsymbol{k}$	Number of consumers
$\boldsymbol{PP^h_{max}}$	Minimum restriction of process-planning data	$\boldsymbol{p_i}$	Predictive value
$\boldsymbol{v_i}$	Iteration velocity	$\boldsymbol{a_i}$	Actual value
$\boldsymbol{t}$	Number of Iteration	$\boldsymbol{MCC}$	The value of Model correlation coefficient
$\boldsymbol{W}$	Matrix of weights, extracted from prediction model	$\boldsymbol{\overline{p}}$	Average value of the predictive values
$\boldsymbol{w_0}$	Inertia weight	$\boldsymbol{\overline{a}}$	Average value of the entire actual values
$\boldsymbol{C_1}$	Cognitive factor 1		

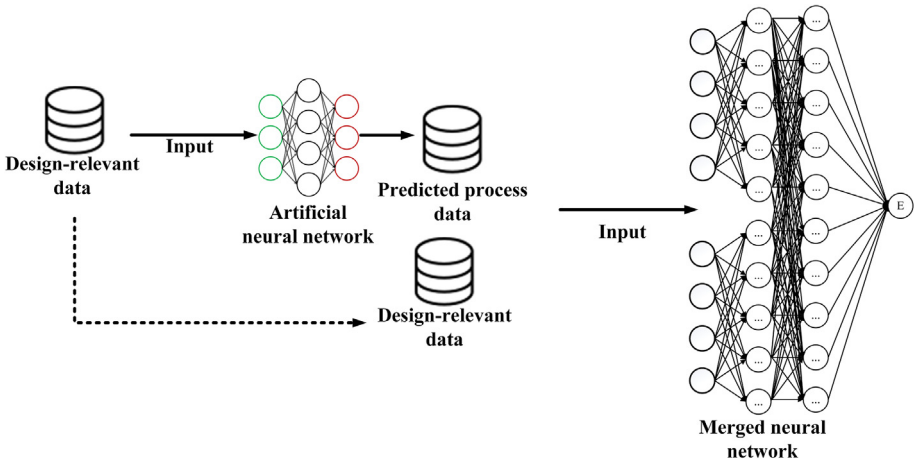

Fig. 1. This figure displays the proposed energy consumption modelling process using the design-relevant data.

$$v_i(t+1) = W*(w_0 * v_i(t) + C_1 * [p_{best}(t) - D_i(t)] + C_2 * [g_{best}(t) - D_i(t)] \times) \tag{7}$$

$$D_i(t+1) = D_i(t) + v_i(t) \tag{8}$$

where v_i is the iteration velocity; w_0 is the inertia weight; C_1 and C_2 are cognitive factors. These two factors determine the cognitive speed when the particle is personal best and globe best.

Comparing to the velocity coefficients of the conventional PSO, the DLD-PSO involves new parameters W. W is the matrix of weights which are extracted from the deep learning prediction model (merged neural network $f_m(D_i, L_j)$). It is denoted by the following functions:

$$w_k^e = [w_1, w_2, \ldots w_K] \tag{9}$$

$$W = \left[w_d^1, w_d^2, \ldots w_d^e\right] \tag{10}$$

After training the deep learning model, weights of all neurons (w_k^e) are defined by the optimiser function. K is the total number of neurons in the first layer that is connected to the input layer. Each neuron on the first layer is fully connected to all the neurons on the input layer, which have the number of $e = g + h$ features. Each weight in the W has represented the weight of a feature of the design-relevant dataset. The W is based on the prediction model. It affects one of the most critical factors of PSO, the changing velocity v_i. Once the optimisation process achieves the maximum number of iterations, the process ends, and the global best of the particle is considered as the optimised results. In Section 3.3, the validation methods are presented.

3.3. Evaluation metrics

The understanding of AM energy consumption is helpful to be determined before introducing the evaluation metrics. The energy consumption shows in this study is the unit energy consumption (E_U), which is shown as:

$$E_U = \frac{E_T}{M_T} \tag{11}$$

where M_T is the product weight of a total build. E_T represents the total energy consumption of each build, which is denoted as following, where j is the number of energy consumers (E_e), such as heating system, layer system, building platform system, and feeding and recycling system, in the system, T is the total time of each process (Qin et al., 2017). It is highlighted that an AM system typically consists of these kinds of consumers, although they may be different in different AM technologies. In addition, when the entire process is considered, involving pre-process and post-process, E_e should include more consumers of pre-process and post-process. In this paper, the energy consumers (E_e) focus on the energy consumers in the AM system (Yosofi et al., 2019).

$$E_T = \sum_j \left(\int_0^T E_e \right) \tag{12}$$

In this study, the model performance is mainly evaluated by Root-mean-square-error (RMSE) and Model correlation coefficient (MCC). The RMSE is used to measure the difference between the predictive value and the actual value, which denotes as:

$$e_{RMSE} = \sqrt{\frac{\sum_{i=1}^{n} (p_i - a_i)^2}{n}} \tag{13}$$

where p_i is the predictive value, a_i is the actual value that is the unit energy of each build (E_U) in this research (Han et al., 2011).

Another performance validation method is the MCC, represented as:

$$MCC = \frac{S_{PA}}{\sqrt{S_P S_A}} \tag{14}$$

$$S_{PA} = \frac{\sum_i (p_i - \overline{p})(a_i - \overline{a})}{n-1}; S_P = \frac{\sum_i (p_i - \overline{p})^2}{n-1}; S_A = \frac{\sum_i (a_i - \overline{a})^2}{n-1} \tag{15}$$

where $\overline{p}$ is the average value of the predictive values, and $\overline{a}$ is the average value of the entire actual values. In Section 4, a case study is introduced, which includes the energy consumption modelling, prediction, and optimisation for an SLS system. The results are revealed by showing the performance of the proposed methods.

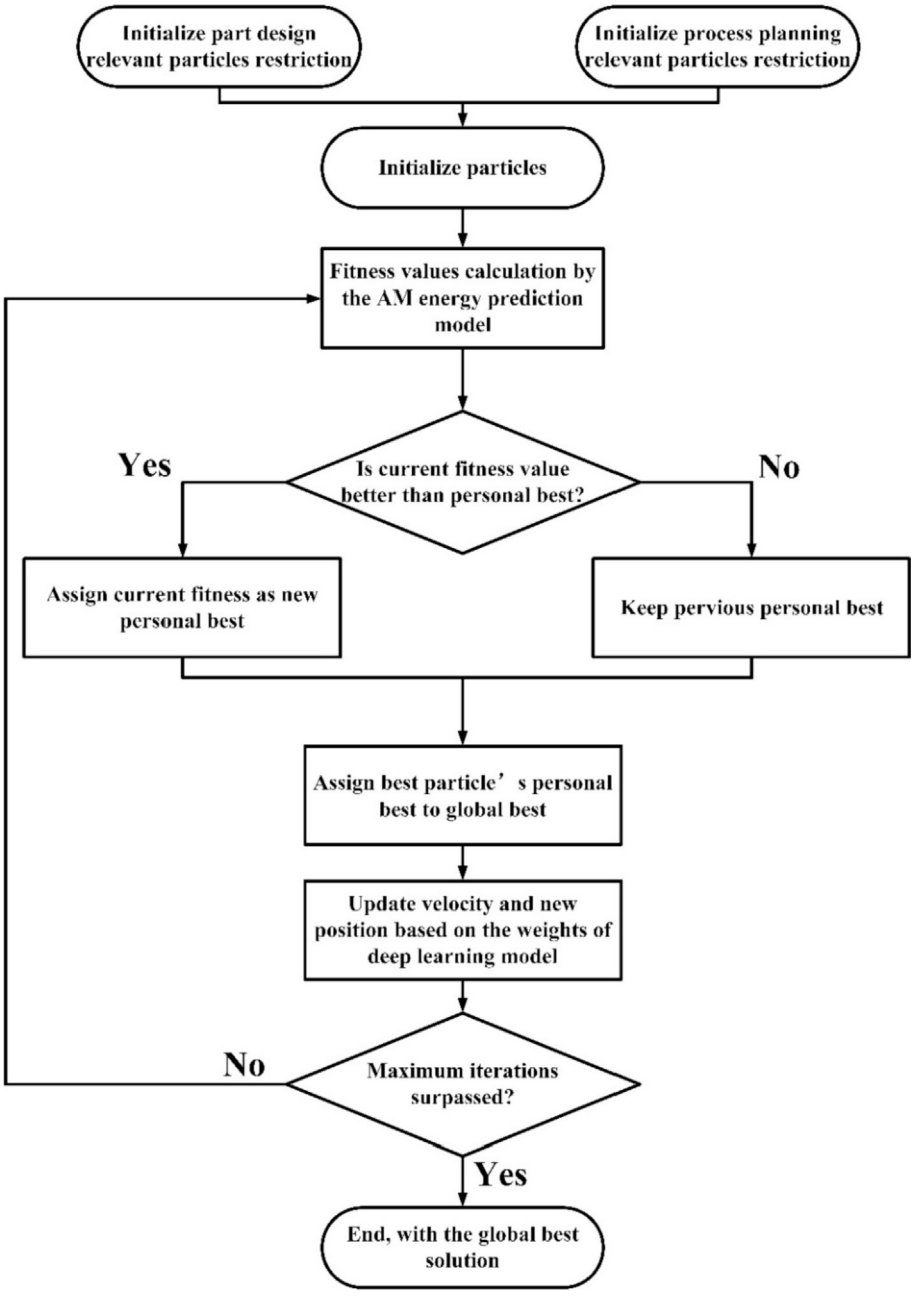

Fig. 2. This flow chart displays the process of the proposed PSO which is driven by deep learning technology.

4. Case study

4.1. Experimental setup

4.1.1. Design-relevant data and target AM system

In this case study, a selective laser sintering (SLS) system (EOS P700) was focused as the target system. The SLS system uses the laser to sinter powder of non-metallic material for producing the parts in a reasonable build chamber size (740 * 400 * 590 mm) (Sreenivasan and Bourell, 2010). The data, used in this case study, had been collected from the target system from August 2016 to December 2018. The entire dataset includes more than a hundred production processes and thousands of parts. These parts were ordered by different companies and designed by various part designers. Each production process produced a wide range of parts in terms of geometric profiles. Also, these parts were placed in different locations with various orientations which were generally determined by operators. These decisions normally depended on system operators' experiences of AM process planning.

It is obvious that every build of this AM process can be very different, in terms of not only the part quantity and geometric profiles but also the process planning factors, such as part position and rotation. In this case study, twelve design-relevant features were extracted to describe the produced models. Table 2 has shown the names and descriptions of these design-relevant features. The original data of these design-relevant features was extracted from the CAD models using the AM design software, Autodesk Netfabb. These features were divided into two classes, the part-design features, and the process-planning features. The part-design features were determined by part designers, and the process-planning

Table 2
The table shows the design-relevant feature description, which includes two types of features, part-design features, and process-planning features.

Part-design features		Process-planning features	
Feature names	Feature description	Feature names	Feature description
Part filling degree (%)	The average ratio between the actual volume and the envelope volume of each part.	Total filling degree (%)	The ratio between the actual volume and the envelope volume of the whole build.
Geometry ratio (wl)	The average ratio between the width and length of each part.	Total geometry ratio (wl)	The ratio between the width and length of each part.
Geometry ratio (hl)	The average ratio between the height and length of each part.	Total geometry ratio (hl)	The ratio between the height and length of the whole build.
		Total geometry ratio (wh)	The ratio between the width and height of each part.
Geometry ratio (wh)	The average ratio between the width and height of each part.	Bottom area (cm^2)	The bottom area of the whole build.
		Height (mm)	The height of the whole build.
Part height (mm)	The average height of each part.	Number of Parts	The total number of parts of the whole build.

features were determined by process operators. When the part designers and process operators decided the part design and the building layout (process plan), these features were defined. Specifically, the part filling degree, the average geometry ratios of three dimensions, and the average part height are the part-design features. The totally filling degree of the whole build, the total geometry ratio of three dimensions, the bottom area, the height of the build, and the number of produced parts are the process-planning features.

Additionally, the basic statistic information of this dataset is shown in Table 3, including the value of the maximum, minimum, average, and standard deviation for each design-relevant feature. These design-relevant features can represent the behaviours of the part designers and the process operators. Furthermore, the target AM process has included a wide range of design-relevant feature and energy consumption. It is interesting to note that the standard deviation of the ratio between the width and the length of the whole build is only 0.0303. The reason is that the AM process operators generally filled the bottom of the building plate entirely. When the build chamber is fully filled, the ratio between the chamber width and its length is about 0.66. More details relevant to the part design and the process operation behaviours are discussed in the Discussion.

4.1.2. AM built examples for optimisation

The actual energy consumptions frequency histogram is displayed in Fig. 3. It is noticeable that over 80% builds consume the unit energy from 120 wh/g to 600 wh/g. However, the energy consumption of each build shows differently even in this range. The standard deviation is 496.8285 wh/g which is larger than the average (about 450 wh/g).

Due to the computing capability, it is necessary to select different examples from the entire range of energy consumption for the simulation. In order to display the reasonable and convincing optimised results, this case study selects four examples that have different energy consumption, which were the Build No. 1 (111.3531 wh/g), Build No. 2 (427.1967 wh/g), Build No. 3 (632.4544 wh/g), and Build No. 4 (1514.6010 wh/g). The design-relevant data of these four examples is shown in Table 4, and the CAD models are displayed in Fig. 4.

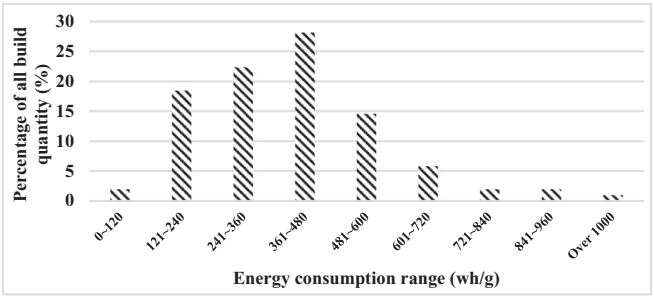

Fig. 3. This histogram shows the energy consumptions range of the entire dataset.

4.1.3. Optimisation restriction

Before introducing the results, the design-relevant feature restrictions are examined. The restrictions are theoretically determined by part designers, process operators, and process capability. According to the interviews of the part designers, and the operators of the target AM process, the historical data and process capability, the restrictions of all features for the four optimised examples are displayed in Table 5. It still gives the part designers and the AM process operators a wide range of choices to optimise their decision for reducing energy consumption.

Moreover, some parameter settings of the neural networks and optimisation algorithms are determined before display the results. All neural networks used two types of activations: 1) for the output layer, scaled exponential linear activation was applied, and 2) for the remaining layers, the rectified linear unit activation was used. The mean squared error was used to represent the loss. Supported by a popular Python package, Keras, the Adam optimiser was used

Table 3
The table presents the basic statistic information of the entire design-relevant dataset.

	Part filling degree (%)	Geometry ratio (wl)	Geometry ratio (hl)	Geometry ratio (wh)	Part height (mm)	Total filling degree (%)	Total geometry ratio (wl)	Total geometry ratio (hl)	Total geometry ratio (wh)	Bottom area (cm^2)	Height (mm)	Number of Part	Energy (wh/g)
Minimum	2.1237	0.0713	0.0319	0.2637	15.4958	1.4895	0.4664	0.0461	0.6448	1228.4154	29.5429	2	107.2829
Maximum	41.4006	7.8088	8.3898	28.1925	321.0955	22.7305	0.6530	0.8246	10.8877	2655.0434	570.6848	115	3468.4256
Average	15.9732	1.1709	0.5615	3.3402	65.4453	8.6514	0.5361	0.2688	2.9369	2359.5735	180.2767	27	483.1233
Standard deviation	9.1083	1.0374	0.8547	3.7172	48.0987	4.5723	0.0303	0.1642	2.1445	295.5327	114.5861	22	496.8285

Table 4
This table shows the original design-relevant feature values and the energy consumption of four build examples.

Build No.	Part filling degree (%)	Geometry ratio (wl)	Geometry ratio (hl)	Geometry ratio (wh)	Part height (mm)	Total filling degree (%)	Total geometry ratio (wl)	Total geometry ratio (hl)	Total geometry ratio (wh)	Bottom area (cm^2)	Height (mm)	Number of Part	Energy (wh/g)
Build No. 1	25.2876	1.2242	0.9478	1.2916	76.4834	12.6910	0.5360	0.3116	1.7202	2558.3574	215.2757	27	111.3531
Build No. 2	17.1347	0.6876	0.1508	4.5597	31.1093	6.6278	0.5420	0.2178	2.4883	2466.3961	146.9372	30	427.1967
Build No. 3	5.4582	0.9810	0.1761	5.5715	44.0349	4.9138	0.5401	0.6390	0.8452	2613.2170	444.4750	33	632.4544
Build No. 4	41.4006	0.9381	0.2662	3.5245	21.1145	5.2255	0.5270	0.1190	4.4278	2476.9831	81.6000	26	1514.6005

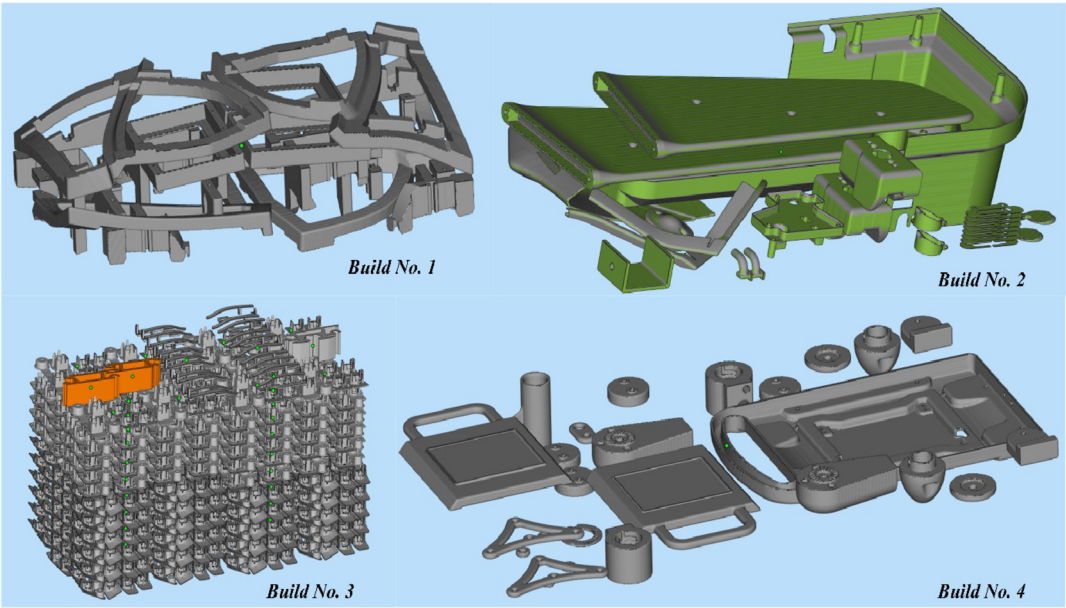

Fig. 4. The figure illustrates the CAD models of four build examples, and each example includes multiple produced parts.

Table 5
The table displays restrictions of the design-relevant features in the four optimised build examples, which are determined by part designers, process operators, and process capability.

Features	Build No. 1	Build No. 2	Build No. 3	Build No. 4
Part filling degree (%)	23.0–28.0	15.0–20.0	3.0–8.0	39.0–44.0
Geometry ratio (wl)	1.0–1.5	0.4–0.9	0.7–1.2	0.6–1.1
Geometry ratio (hl)	0.7–1.2	0.05–0.55	0.05–0.55	0.05–0.55
Geometry ratio (wh)	1.0–1.5	4.3–4.8	5.3–5.8	3.3–3.8
Part height (mm)	60–90	22.5–52.5	35.0–48.0	18.0–38.0
Total filling degree (%)	10.0–15.0	5.0–10.0	3.0–8.0	3.0–8.0
Total geometry ratio (wl)	0.3–0.8	0.3–0.8	0.3–0.8	0.3–0.8
Total geometry ratio (hl)	0.1–0.6	0.1–0.6	0.4–0.9	0.05–0.55
Total geometry ratio (wh)	1.5–2.0	2.2–2.7	0.6–1.1	4.2–4.7
Bottom area (cm^2)	2000–3000	2000–3000	2000–3000	2000–3000
Height (mm)	195–270	143–225	420–495	75–100
Number of Part	15–35	20–40	23–43	16–36

(LeCun et al., 2015b). Based on the dimension of input data, the participles pool size is 100, and the maximum number of iterations is 1000 for the PSOs in this paper (Röhler and Chen, 2011). Basic parameters of the conventional PSO, i.e., constriction coefficient 1 (c_1), constriction coefficient 2 (c_2), and inertia weight (w_o), are 2, 2, 0.748 respectively, which is commonly used in PSO applications (Yusup et al., 2012).

In Section 4.2, the results of the case study are reported and discussed. Firstly, the results of the energy consumption prediction model are presented to show the merits of the proposed prediction method. Secondly, the comparison between the proposed and conventional PSO is explained. Also, optimisation of four example

builds is presented by showing the details of the optimised features.

4.2. Results

4.2.1. Energy consumption prediction

Based on the validation metrics that are shown in Section 3.3, the results of three energy prediction models, which are the ANN model using design-relevant data directly, the proposed model, and the multi-source data model, are displayed in Table 6. The proposed model is compared to our previous energy consumption prediction model (Qin et al., 2018) and the model that only uses design-relevant data. The MCC of the proposed energy consumption model that is introduced in this paper is 0.7908, and RSME is 23.2163 wh/g. According to the previous work (Qin et al., 2018), the MCC of the energy consumption prediction model using multi-source data is 0.8030, and the RSME is 20.2271 wh/g. The comparison of the proposed model and the previous model reveal that, although the proposed method has not obtained the best results, it is still acceptable with only 0.0122 MCC and 2.9892 wh/g RSME difference. It is highlighted that the RSME of the proposed model is twice less than the model using an ANN model to predict energy consumption. Furthermore, the proposed model is better than the benchmark models that were compared in the previous paper. The performances of benchmark models are shown in the previous paper, which the MCC and the RMSE of the Linear regression are 0.607 and 115.056 wh/g; the MCC and the RMSE of the Decision tree are 0.691 and 59.585 wh/g; the MCC and the RMSE of the *k*-nearest neighbours are 0.541 and 44.168 wh/g (Qin et al., 2018).

Moreover, the weights of the design-relevant feature are extracted from the merged neural networks. The weights displayed in Table 7. The most substantial one (0.1254) is the weight of the total filling degree. Also, there exist other four weights which are higher than the average weight, the geometry of width and height, the bottom area, the height of the whole build, and the geometry of height and length. These five features are considered as the most critical features that can significantly impact the prediction of AM energy consumption in this case study.

In addition, Table 8 shows the comparison between predictive energy consumption and the actual energy consumption for these four builds. The absolute average error of these builds is about 34.3513 wh/g, which is close to the RSME of the proposed model (23.2163 wh/g). The error will grow when the energy consumption increases. The lowest prediction error (+4.9959 wh/g) is from Build No. 1, while the actual energy consumption is 111.3531 wh/g. The largest error (−78.2030 wh/g) of these four examples is Build No. 4, while the actual energy consumption is 1514.6010 wh/g.

4.2.2. The comparison between the DLD-PSO and the conventional PSO

Three types of optimisation results are presented depending on the decision of part designers and operators. The part-designer-oriented optimisation is for AM part designer only. The process-operator-oriented optimisation is to optimise the process operators' decision. The designer-and-operator-oriented optimisation considers optimising the decisions of part designers and process operators. Fig. 5, Fig. 6, Fig. 7, and Fig. 8 display the optimisation results of four build examples using the conventional PSO and the DLD-PSO. Among these optimisation results, the proposed PSO generally obtains better results that require lower energy consumption than the conventional PSO in smaller convergence time.

Table 9 shows the optimisation performance of the conventional and the DLD-PSO including the convergence speed, I_v (iteration), and the lowest energy consumption, E_l (wh/g). The average

Table 6
This table shows the prediction result comparison of proposed modelling, previous modelling, and ANN modelling.

Prediction model	MCC	RSME
ANN model using design-relevant data	0.7012	69.5732 wh/g
Proposed energy consumption prediction model	**0.7908**	**23.2163 wh/g**
Multi-source data predict energy consumption (Qin et al., 2018)	0.8030	20.2271 wh/g

Bold values indicate the highest MCC value and the lowest RSME value.

Table 7
The table presents the weights of all design-relevant features, including two types of design-relevant features, extracted from the merged neural networks.

Part-design features		Process-planning features	
Feature name	Weight	Feature name	Weight
Part filling degree (%)	0.074412	Total filling degree (%)	**0.1209025**
Geometry ratio (wl)	0.082751	Total geometry ratio (wl)	0.066752
Geometry ratio (hl)	0.084189	Total geometry ratio (hl)	0.069722
		Total geometry ratio (wh)	0.07202
Geometry ratio (wh)	0.095772	Bottom area (cm^2)	0.085395
		Height (mm)	0.083247
Part height (mm)	0.079321	Number of Parts	0.085492
Total weight	**0.416445**		**0.5835305**

Bold values indicate the largest weight value and the total weight values of two types of design relevant features.

Table 8
The table displays the comparison between the predictive and the actual energy consumption for four build examples with error values.

	Build No. 1	Build No. 2	Build No. 3	Build No. 4
Actual energy consumption (wh/g)	111.3531	427.1967	632.4544	1514.6010
Predictive energy consumption (wh/g)	116.3490	408.2854	597.1588	1436.3987
Error (wh/g)	**+4.9959**	−18.9113	−35.2956	−78.2023

Bold value indicates the lowest error.

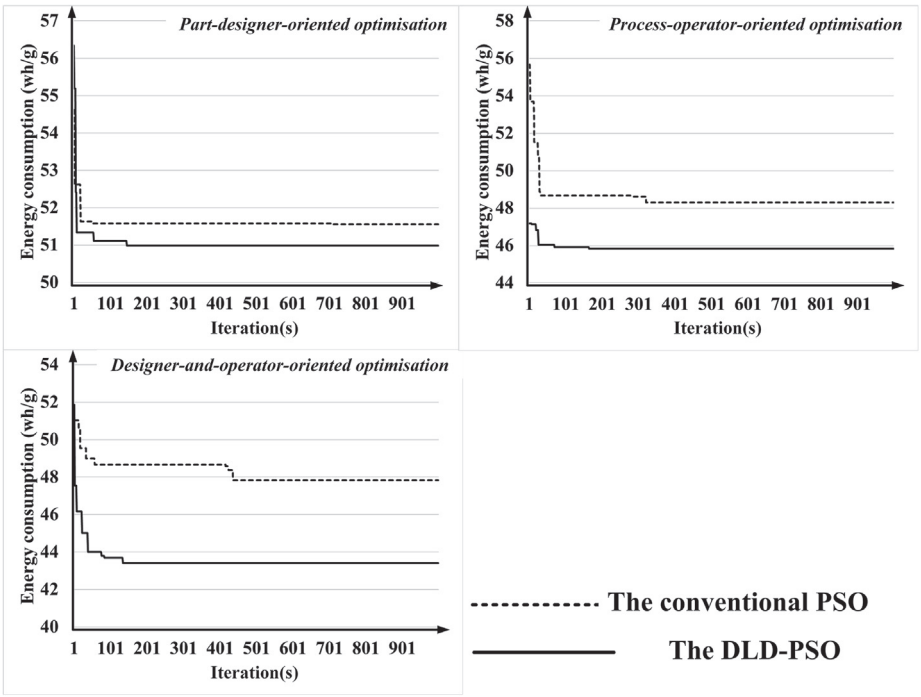

Fig. 5. This figure shows three types of optimisation processes of the conventional and the DLD-PSO for Build No. 1.

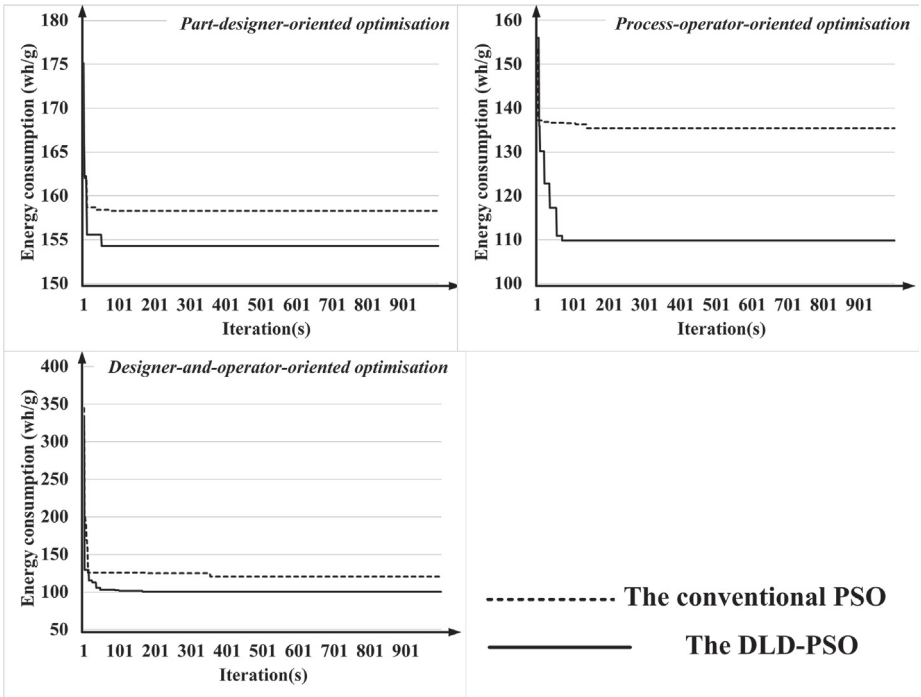

Fig. 6. This figure shows three types of optimisation processes of the conventional and the DLD-PSO for Build No. 2.

convergence iteration of the conventional PSO is 360 iterations which are significantly larger than the proposed PSO (114 iterations). With the help of deep learning-driven weights, the proposed PSO is able to search the globe best faster than the conventional PSO which uses the constant cognitive factors to determine the convergence speed. It is interesting to note that in comparison with each optimisation based on the DLD-PSO, the part-designer-oriented optimisation obtains the best results within the minimal iteration, 82 iterations on average, and process-operator-oriented optimisation have spent the more time to get the best results, 134 iteration on average. Moreover, the DLD-PSO optimised energy consumption is generally lower than the conventional PSO optimised energy consumption, which is about 2.14% for the part-designer-oriented optimisation, about 6.62% for the process-operator-oriented optimisation, and about 3.40% for the designer-and-operator-oriented optimisation.

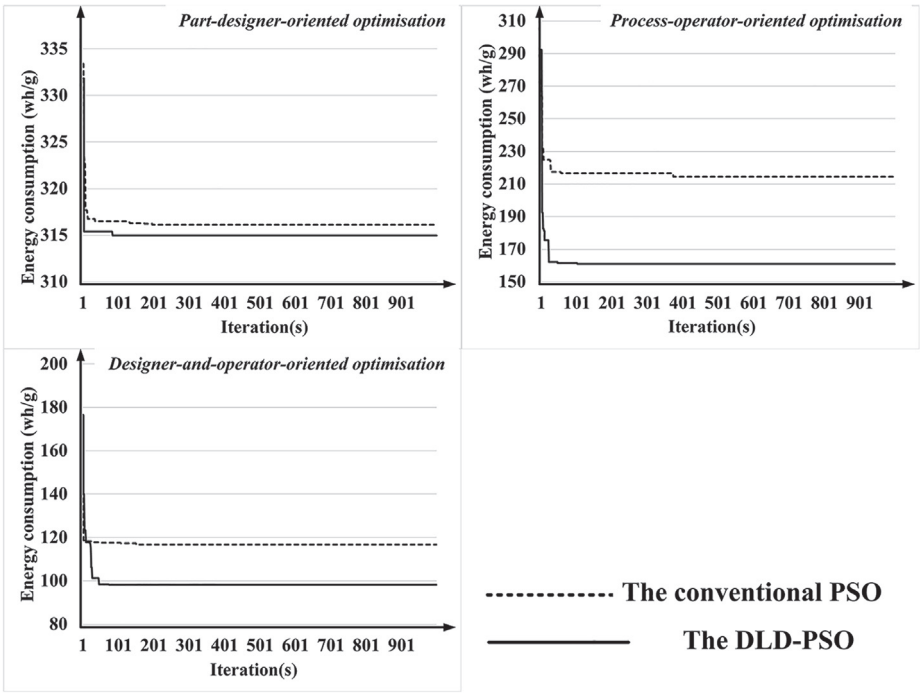

Fig. 7. This figure shows three types of optimisation processes of the conventional and the DLD-PSO for Build No. 3.

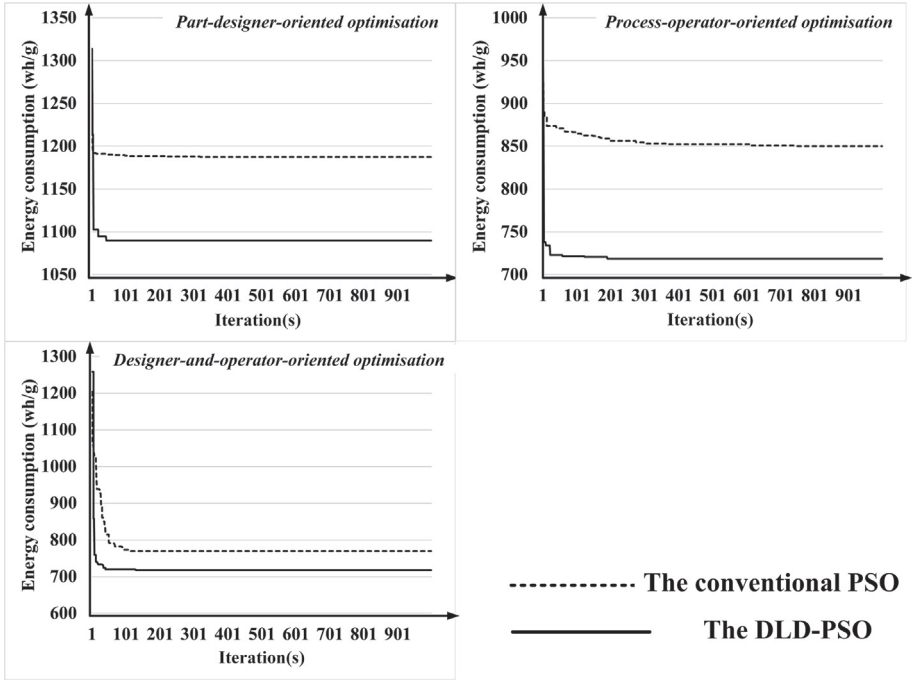

Fig. 8. This figure shows three types of optimisation processes of the conventional and the DLD-PSO for Build No. 4.

Table 9
This table displays the results (convergence speed and lowest energy consumption) of three types of optimisation using the conventional PSO and DLD-PSO.

		Build No. 1		Build No. 2		Build No. 3		Build No. 4	
		I_v	E_l (wh/g)	I_v	E_l (wh/g)	I_v	E_l (wh/g)	I_v	E_l (wh/g)
Conventional PSO	Part-designer- oriented optimisation	713	51.5563	147	158.2691	493	316.1101	396	1187.2131
	Process-operator-oriented optimisation	323	48.3003	139	135.4456	375	214.3041	611	850.5141
	Designer-and-operator-oriented optimisation	425	48.3733	355	120.8380	153	116.6745	188	*769.9511*
DLD-PSO	Part-designer- oriented optimisation	147	50.9837	52	154.2734	85	314.3977	44	1089.6268
	Process-operator-oriented optimisation	166	45.8434	72	109.7810	104	160.9628	192	718.8854
	Designer-and-operator-oriented optimisation	136	**43.4054**	166	**100.4880**	76	**98.1448**	132	**717.8302**

Bold values indicate the lowest energy consumption values of four examples.

Table 10
This table displays the optimised results including design-relevant feature optimisation and the reduced energy for Build No.1 which the original unit energy consumption is 111.3531 wh/g.

		Part filling degree (%)	Geometry ratio (wl)	Geometry ratio (hl)	Geometry ratio (wh)	Part height (mm)	Total filling degree (%)	Total geometry ratio (wl)	Total geometry ratio (hl)	Total geometry ratio (wh)	Bottom area (cm^2)	Height (mm)	Number of Part	Energy (wh/g)
I	Optimised results	26.3859	1.2688	0.9897	1.2931	70.94	12.6910	0.5360	0.3116	1.7202	2558.3574	215.28	27	50.9837
	Difference	+1.0983	+0.0446	+0.0419	+0.0015	−5.54	0	0	0	0	0	0	0	−60.3653
II	Optimised results	25.2876	1.2242	0.9478	1.2916	76.48	14.0004	0.4606	0.2907	1.6993	2457.3249	252.52	22	45.8434
	Difference	0	0	0	0	0	+1.3094	−0.0754	−0.0209	−0.0209	−101.0325	+37.24	−5.0000	−65.5056
III	Optimised results	25.1556	1.2020	0.9277	1.3054	79.13	13.9552	0.4469	0.2790	1.7620	2424.4020	225.95	19	**43.4054**
	Difference	−0.1320	−0.0222	−0.0201	+0.0138	+2.64	+1.2642	−0.0891	−0.0326	+0.0418	−133.9554	+10.67	−8	−67.9436
IV	Optimised results	26.3859	1.2688	0.9897	1.2931	70.94	14.0004	0.4606	0.2907	1.6993	2457.3249	252.52	22	48.1260
	Difference	+1.0983	+0.0446	+0.0419	+0.0015	−5.54	+1.3094	−0.0754	−0.0209	−0.0209	−101.0325	+37.2443	−5	−63.2230

Bold value indicates the lowest energy consumption values of four examples.

4.2.3. Optimisation details

Table 10 to Table 13 show all optimisation results of the DLD-PSO which include the part-designer-oriented optimisation, initialized as *I*, the process-operator-oriented optimisation, initialized as *II*, and the designer-and-operator-oriented optimisation, initialized as *III*. In addition, Tables 10–13 include another set of optimised result, initialized as *IV*. The energy consumption of *IV* is calculated by the proposed prediction model through the optimised design-relevant features from *I* and *II*. It is highlighted that the proposed PSO is not applied to generate *IV*. Generally, the most substantial reduction of AM energy consumption appears in the designer-and-operator-oriented optimisation for these four build examples, which reduces the energy usage by 67.92%. Comparing four examples, the most substantial reduction of AM energy consumption is on Build No. 3, 83.57% energy usage is reduced in the designer-and-operator-oriented optimisation. Furthermore, the largest average reduction of AM energy consumption reduction of three types of optimisation is 70.24% (Build No. 2). Also, the energy consumption reduction of the optimisation *IV* is generally smaller than the designer-and-operator-oriented optimisation.

In Tables 10–13, the most considerable change of the optimised design-relevant feature is the total filling degree, which has changed 45.64% in the process-operator-oriented optimisation and about 38.43% in the designer-and-operator-oriented optimisation. The weight of the total filling degree (0.121) is also the largest compared to the weights of other features. Moreover, the changes in the part-designer-oriented and the process-operator-oriented optimisation are generally more significant than the changes of the designer-and-operator-oriented optimisation. It is interesting to note that the changes in the optimised design-relevant-features grow when original energy consumption increases. specifically, Build No. 1 cost the lowest energy consumption (116.3490 wh/g), and the average change of all features is about 14.39%. In contrast, the most substantial feature change is Build No. 4, which is about 27.29%.

5. Discussion

5.1. Discussion on results

In the case study, the proposed design-relevant based AM energy consumption modelling and optimisation approach were validated. The algorithm performance of the proposed approach, in terms of MCC and RMSE, is acceptable—1.52% MCC lower and 4.98% RSME higher—although it was not better than the performance of the multi-source data prediction model. However, the multi-source data prediction model also involves data collected during the AM process, which cannot be used in optimisation. Also, the proposed approach obtained the better results than the simple ANN-based model and other benchmark algorithms, linear regression, decision tree and *k*-nearest neighbours, which were used in previous works (Qin et al., 2018).

In the validation of the optimisation performance, four build examples with various energy costs were examined in the case study. The design-relevant features were categorised as two classes: the part-design features, and process-planning features. For optimal results, each feature of these two classes was changed within restriction ranges that were determined by part designers and process operators. The restriction ranges in this case study were determined by part designers, process operators, and SLS process capabilities. It provided these groups of professionals a reasonable range in which to optimise decisions regarding the reduction of AM process energy consumption. Optimisation performance was shown through three types of optimisation oriented toward different professionals.

Table 11
This table displays the optimised results including design-relevant feature optimisation and the reduced energy for Build No.2 which the original unit energy consumption is 427.1967 wh/g.

		Part filling degree (%)	Geometry ratio (wl)	Geometry ratio (hl)	Geometry ratio (wh)	Part height (mm)	Total filling degree (%)	Total geometry ratio (wl)	Total geometry ratio (hl)	Total geometry ratio (wh)	Bottom area (cm^2)	Height (mm)	Number of Part	Energy (wh/g)
I	Optimised results	16.0894	0.5962	0.3819	4.4716	37.74	6.6278	0.5420	0.2178	2.4883	2466.3961	146.94	30	154.2734
	Difference	−1.0453	−0.0914	+0.2311	−0.0881	+6.63	0	0	0	0	0	0	0	−272.9233
II	Optimised results	17.1347	0.6876	0.1508	4.5597	31.11	9.3045	0.5074	0.3162	2.3265	2714.9799	180.05	22	109.7810
	Difference	0	0	0	0	0	+2.6767	−0.0346	+0.0984	−0.1618	+248.5838	+33.11	−8	−317.7087
III	Optimised results	16.6467	0.7105	0.1352	4.5853	36.07	8.9977	0.5169	0.2724	2.4418	2695.2499	165.63	25	**100.4880**
	Difference	−0.4880	+0.0229	−0.0156	+0.0256	+4.96	+2.3699	−0.0251	+0.0546	−0.0465	+228.8538	+18.69	−5	−326.7087
IV	Optimised results	16.0894	0.5962	0.3819	4.4716	37.74	9.3045	0.5074	0.3162	2.3265	2714.9799	180.05	22	123.9675
	Difference	−1.0453	−0.0914	+0.2311	−0.0881	+6.63	+2.6767	−0.0346	+0.0984	−0.1618	+248.5838	+33.11	−8	−303.2292

Bold value indicates the lowest energy consumption values of four examples.

Table 12
This table displays the optimised results including design-relevant feature optimisation and the reduced energy for Build No.3 which the original unit energy consumption is 632.4544 wh/g.

		Part filling degree (%)	Geometry ratio (wl)	Geometry ratio (hl)	Geometry ratio (wh)	Part height (mm)	Total filling degree (%)	Total geometry ratio (wl)	Total geometry ratio (hl)	Total geometry ratio (wh)	Bottom area (cm^2)	Height (mm)	Number of Part	Energy (wh/g)
I	Optimised results	7.5168	0.7736	0.4717	5.5533	46.60	4.9138	0.5401	0.6390	0.8452	2613.2170	444.48	33	314.3977
	Difference	+2.0586	−0.2074	+0.2956	−0.0182	+2.57	0	0	0	0	0	0	0	−318.0567
II	Optimised results	5.4582	0.9810	0.1761	5.5715	44.03	7.8365	0.6876	0.4480	0.8012	2698.5380	435.46	29	160.9628
	Difference	0	0	0	0	0	+2.9227	+0.1475	−0.1910	−0.0440	+85.3210	−9.02	−4	−471.4916
III	Optimised results	4.1210	0.8763	0.2750	5.5370	44.96	7.3646	0.6292	0.4460	0.8084	2654.8710	443.05	30	**98.1448**
	Difference	−1.3372	−0.1047	+0.0989	−0.0345	+0.93	+2.4508	+0.0891	−0.1930	−0.0368	+41.6540	−1.43	−3	−534.3096
IV	Optimised results	7.5168	0.7736	0.4717	5.5533	46.60	7.8365	0.6876	0.4480	0.8012	2698.5380	435.46	29	101.04134
	Difference	+2.0586	−0.2074	+0.2956	−0.0182	+2.57	+2.9227	+0.1475	−0.1910	−0.0440	+85.3210	−9.02	−4	−531.4131

Bold value indicates the lowest energy consumption values of four examples.

Table 13
This table displays the optimised results including design-relevant feature optimisation and the reduced energy for Build No.4 which the original unit energy consumption is 1514.6010 wh/g.

		Part filling degree (%)	Geometry ratio (wl)	Geometry ratio (hl)	Geometry ratio (wh)	Part height (mm)	Total filling degree (%)	Total geometry ratio (wl)	Total geometry ratio (hl)	Total geometry ratio (wh)	Bottom area (cm^2)	Height (mm)	Number of Part	Energy (wh/g)
I	Optimised results	39.5530	0.8958	0.0878	3.4442	27.71	5.2255	0.5270	0.1190	4.4278	2476.9831	81.60	26	1089.6268
	Difference	−1.8476	−0.0423	−0.1784	−0.0803	+6.60	0	0	0	0	0	0	0	−424.9742
II	Optimised results	41.4006	0.9381	0.2662	3.5245	21.11	7.4449	0.6627	0.3207	4.3755	2725.8123	112.66	32	718.8854
	Difference	0	0	0	0	0.00	+2.2194	+0.1357	+0.2017	−0.0523	+248.8292	+31.06	+6	−795.7156
III	Optimised results	39.9526	0.9038	0.3158	3.6697	25.65	6.8276	0.7046	0.2283	4.3160	2721.7830	121.35	33	**717.8302**
	Difference	−1.4480	−0.0343	+0.0496	+0.1452	+4.54	+1.6021	+0.1776	+0.1093	−0.1118	+244.7999	+39.75	+7	−796.7708
IV	Optimised results	39.5530	0.8958	0.0878	3.4442	27.71	7.9975	0.7987	0.5500	4.4408	2987.9628	102.53	36	847.1742
	Difference	−1.8476	−0.0423	−0.1784	−0.0803	+6.60	+2.7720	+0.2717	+0.4310	+0.0130	+510.9797	+20.93	+10	−667.4268

Bold value indicates the lowest energy consumption values of four examples.

Generally, the DLD-PSO model obtains the best results faster than conventional PSO method do, in terms of faster convergence speed and lower energy consumption. Moreover, the best results of this model, in terms of lowest energy consumption, were lower than those of the conventional PSO model. The process-operator-oriented optimisation through the DLD-PSO model offered a significant improvement over the conventional PSO. It can be seen from the results that the weights of each feature in the deep learning-based prediction model represent the impacts of these features on the target value which is energy consumption in this study. Additionally, the weights driven by the deep learning-based model can help the PSO model find better results faster than conventional PSO model.

Three types of optimisation were generated in this case study, process-operator-oriented optimisation obtained better results than part-designer-oriented optimisation did. This may be caused

by the seven features were changed in process-operator-oriented optimisation, and one of them had the largest weight of all the features. Furthermore, designer-and-operator-oriented optimisation consumed the lowest amount of energy—an amount lower than that of part-designer-oriented optimisation and process-operator-oriented optimisation combined (optimisation *IV*). This means that design-relevant features and energy consumption are not independent of each other in this optimisation method. When an optimisation method accounts for all design-relevant features, the lowest possible energy consumption can be obtained. This requires the cooperation of AM part designers and process operators, which is the main principle of DfAM (Thompson et al., 2016). Though these two groups of professionals work separately, AM energy consumption can still be reduced using the proposed optimisation method. Currently, when part designers and process operators made decisions they may have not realised the relationship between energy consumption and these design-relevant features yet. However, with the development of the research, these design-relevant features will be highlighted in the AM design software for reducing AM energy consumption in the future.

5.2. Discussion on the proposed approach and future works

In this paper, AM energy consumption was predicted using a deep learning-based prediction model. Different from the previous work, the model, built in this paper, used design-relevant data derived from multi-source data of AM systems. The data was collected before the AM process began, which indicates that AM energy consumption is predicted prior to the production process commencing. Comparing to our previous study, the modelling and prediction method proposed in this paper has been improved, which provides an opportunity to understand and reduce the AM energy consumption before the process.

Other relevant researches in the literature review generally focused on the impacts of one or two design-relevant features, such as the filling structure and part orientation. They examined the relationship between these impacts and energy consumption through the experiments focusing on certain values of these features. However, with the rapid development of AM technology, AM tends to produce multiple parts in one production, especially for SLS and SLM systems (Chergui et al., 2018). It is hard to analyse the system only based on the one or two features that descript the single part, like part orientation. Also, the part produced in AM generally is complex because of the special structure and design. Therefore, it is necessary to consider more design features, which can represent the design information precisely. In addition, only applying the experiment is difficult to validate this complex issue that should involve significant varies of each feature. Comparing to the other relevant researches reviewed in Section 2, the proposed approach involves more AM design-relevant features, including part-design features and process-planning features, which are able to represent the design condition of multiple part production. These two types of design-relevant features are proposed based on the review of DfAM research, which stands on both perspectives of part designer and process operators. Furthermore, the proposed method was built and validated by a large sum of historical data, including thousands of CAD models in over a hundred builds. Different from other relevant studies, this method covers much more variables of each feature according to the actual production.

The proposed method is a data-driven approach which is highly depended on the historical data. Although different AM technologies may have different working mechanisms and principles, the approach in exploiting such data so to facilitate its process modelling and analytics remain similar. In addition, the data required in this research can be generally collected from other AM processes based on the method proposed in this study, or the collected data can be converted to the same data characteristic to match the input requirement. In practice, this research has been collecting the data from 1 a.m. system for more than two years, including processing data, material condition information and CAD model information. It will not only raise the cost of the research but also extend the research time to build the model based on another AM system. However, benefitting from the increasingly completed monitoring system and Internet of Thing (IoT) technologies, the AM system is collecting more and more data from the process and related objects. In the future, this method will be validated on other AM technologies to prove its generality. Moreover, two types of design-relevant features are used in this research, which has not covered the entire area of DfAM. Another future work in this research is to collect more design-relevant data. For example, the material design can be one type of important feature due to the multiple material AM production is a trend in both academia and industry (Thompson et al., 2016). Furthermore, testing experiments should be applied to validate the simulation results in the future.

6. Conclusions

Energy consumption has become a significant issue in AM processes. The focus of this paper has been on the optimisation of AM process energy consumption which is also based on the data-driven modelling and prediction. The proposed optimisation approach was inspirited by a review of related research indicating the significance of DfAM and PSO in the manufacturing domain. An energy consumption prediction approach based on deep learning technology has been proposed that uses design-relevant data as input. Design-relevant data is generated before the AM process begins and includes part design data and process planning data, which are determined by part designers and process operators. Furthermore, in order to reduce AM energy consumption, the DLD-PSO approach is proposed to optimise design-relevant features. A case study showing the merits of the proposed approach was carried out based on SLS process data. It appears that the proposed energy consumption prediction approach obtained results similar to those of the previous multi-source data prediction model. For optimisation purposes, three types of optimisation oriented toward different groups of professionals were introduced. It was found that the DLD-PSO model yields a greater convergence speed and lower energy consumption than the conventional PSO. Four build examples were adopted to validate the proposed optimisation method. The best results were obtained to generate the recommendations for part designers and process operators. Finally, this approach is a data-driven approach which can be also developed to help other AM technologies.

Acknowledgments

The work described in this paper was partially supported by the National Natural Science Foundation of China (51675388), the 2018 Green Manufacturing System Integration project funded by the Ministry of Information Industry China, and the China Scholarship Council (CSC) through a PhD scholarship (20160806238). These financial contributions are gratefully acknowledged.

References

Bai, Q., 2010. Analysis of particle swarm optimization algorithm. Comput. Inf. Sci. 3, 180.

Baumers, M., Tuck, C., Bourell, D.L., Sreenivasan, R., Hague, R., 2011a. Sustainability of additive manufacturing: measuring the energy consumption of the laser sintering process. Proc. Inst. Mech. Eng. B J. Eng. Manuf. 225, 2228–2239.

Baumers, M., Tuck, C., Wildman, R., Ashcroft, I., Hague, R., 2011b. Energy inputs to

additive manufacturing: does capacity utilization matter. Eos 1000, 30–40.
Bensingh, R.J., Machavaram, R., Boopathy, S.R., Jebaraj, C., 2019. Injection molding process optimization of a bi-aspheric lens using hybrid artificial neural networks (ANNs) and particle swarm optimization (PSO). Measurement 134, 359–374.
Chen, S.-M., Huang, Z.-C., 2017. Multiattribute decision making based on interval-valued intuitionistic fuzzy values and particle swarm optimization techniques. Inf. Sci. 397–398, 206–218.
Chergui, A., Hadj-Hamou, K., Vignat, F., 2018. Production scheduling and nesting in additive manufacturing. Comput. Ind. Eng. 126, 292–301.
Ding, Z., Jiang, Z., Zhang, H., Cai, W., Liu, Y., 2018. An integrated decision-making method for selecting machine tool guideways considering remanufacturability. Int. J. Comput. Integr. Manuf. 1–12.
Eyers, D.R., Potter, A.T., 2017. Industrial Additive Manufacturing: a manufacturing systems perspective. Comput. Ind. 92–93, 208–218.
Gardan, N., Schneider, A., 2015. Topological optimization of internal patterns and support in additive manufacturing. J. Manuf. Syst. 37, 417–425.
Gebisa, A.W., Lemu, H.G., 2017. Design for manufacturing to design for Additive Manufacturing: analysis of implications for design optimality and product sustainability. Procedia Manuf. 13, 724–731.
Gibson, I., Rosen, D.W., Stucker, B., 2010. Design for Additive Manufacturing, Additive Manufacturing Technologies. Springer, pp. 299–332.
Han, J., Kamber, M., Pei, J., 2011. Data Mining: Concepts and Techniques. Elsevier.
Huang, S.H., Liu, P., Mokasdar, A., Hou, L., 2013. Additive manufacturing and its societal impact: a literature review. Int. J. Adv. Manuf. Technol. 67, 1191–1203.
Janahiraman, T.V., Ahmad, N., Nordin, F.H., 2018. Extreme learning machine and particle swarm optimization in optimizing CNC turning operation. In: IOP Conference Series: Materials Science and Engineering. IOP Publishing, 012086.
Jiang, Z., Ding, Z., Zhang, H., Cai, W., Liu, Y., 2019. Data-driven ecological performance evaluation for remanufacturing process. Energy Convers. Manage. 198, 111844.
Junk, S., Coté, S., 2013. Influencing variables on sustainability in additive manufacturing. Green Des. Mater. Manuf. Process. 167.
Kennedy, J., 2011. Particle Swarm Optimization, Encyclopedia of Machine Learning. Springer, pp. 760–766.
Kim, B.-I., Son, S.-J., 2012. A probability matrix based particle swarm optimization for the capacitated vehicle routing problem. J. Intell. Manuf. 23, 1119–1126.
Kim, S.G., Theera-Ampornpunt, N., Fang, C.-H., Harwani, M., Grama, A., Chaterji, S., 2016. Opening up the blackbox: an interpretable deep neural network-based classifier for cell-type specific enhancer predictions. BMC Syst. Biol. 10, 54.
Kuo, R.J., Lin, L.M., 2010. Application of a hybrid of genetic algorithm and particle swarm optimization algorithm for order clustering. Decis. Support Syst. 49, 451–462.
LeCun, Y., Bengio, Y., Hinton, G., 2015a. Deep learning. Nature 521, 436.
LeCun, Y., Bengio, Y., Hinton, G., 2015b. Deep learning. Nature 521, 436–444.
Li, L., Liu, J., Ma, Y., Ahmad, R., Qureshi, A., 2019. Multi-view feature modeling for design-for-additive manufacturing. Adv. Eng. Inf. 39, 144–156.
Ma, J., Harstvedt, J.D., Dunaway, D., Bian, L., Jaradat, R., 2018. An exploratory investigation of Additively Manufactured Product life cycle sustainability assessment. J. Clean. Prod. 192, 55–70.
Moradi, M.H., Abedini, M., 2012. A combination of genetic algorithm and particle swarm optimization for optimal DG location and sizing in distribution systems. Int. J. Electr. Power Energy Syst. 34, 66–74.
Niaki, M.K., Torabi, S.A., Nonino, F., 2019. Why manufacturers adopt additive manufacturing technologies: the role of sustainability. J. Clean. Prod. 222, 381–392.
Panda, B.N., Garg, A., Shankhwar, K., 2016. Empirical investigation of environmental characteristic of 3-D additive manufacturing process based on slice thickness and part orientation. Measurement 86, 293–300.
Paul, R., Anand, S., 2012. Process energy analysis and optimization in selective laser sintering. J. Manuf. Syst. 31, 429–437.
Peng, T., Kellens, K., Tang, R., Chen, C., Chen, G., 2018. Sustainability of additive manufacturing: an overview on its energy demand and environmental impact. Additive Manuf. 21, 694–704.
Qin, J., Liu, Y., Grosvenor, R., 2017. A framework of energy consumption modelling for additive manufacturing using Internet of things. Procedia CIRP 63, 307–312.
Qin, J., Liu, Y., Grosvenor, R., 2018. Multi-source data analytics for AM energy consumption prediction. Adv. Eng. Inf. 38, 840–850.
Raju, M., Gupta, M.K., Bhanot, N., Sharma, V.S., 2018. A hybrid PSO–BFO evolutionary algorithm for optimization of fused deposition modelling process parameters. J. Intell. Manuf. 1–16.
Röhler, A.B., Chen, S., 2011. An analysis of sub-swarms in multi-swarm systems. In: Australasian Joint Conference on Artificial Intelligence. Springer, pp. 271–280.
Shi, Y., 2001. Particle swarm optimization: developments, applications and resources, evolutionary computation. In: 2001. Proceedings of the 2001 Congress on. IEEE, pp. 81–86.
Sreenivasan, R., Bourell, D., 2010. Sustainability Study in Selective Laser Sintering-an Energy Perspective. Minerals, Metals and Materials Society/AIME, 420 Commonwealth Dr.. P. O. Box 430 Warrendale PA 15086 USA.
Tang, D., Dai, M., Salido, M.A., Giret, A., 2016a. Energy-efficient dynamic scheduling for a flexible flow shop using an improved particle swarm optimization. Comput. Ind. 81, 82–95.
Tang, Y., Mak, K., Zhao, Y.F., 2016b. A framework to reduce product environmental impact through design optimization for additive manufacturing. J. Clean. Prod. 137, 1560–1572.
Tang, Y., Zhao, Y.F., 2016. A survey of the design methods for additive manufacturing to improve functional performance. Rapid Prototyp. J. 22, 569–590.
Thompson, M.K., Moroni, G., Vaneker, T., Fadel, G., Campbell, R.I., Gibson, I., Bernard, A., Schulz, J., Graf, P., Ahuja, B., 2016. Design for additive manufacturing: trends, opportunities, considerations, and constraints. CIRP Annals 65, 737–760.
Verhoef, L.A., Budde, B.W., Chockalingam, C., García Nodar, B., van Wijk, A.J.M., 2018. The effect of additive manufacturing on global energy demand: an assessment using a bottom-up approach. Energy Policy 112, 349–360.
Watson, J.K., Taminger, K.M.B., 2018. A decision-support model for selecting additive manufacturing versus subtractive manufacturing based on energy consumption. J. Clean. Prod. 176, 1316–1322.
Wohlers, T., 2016. Wohlers Report 2016. Wohlers Associates, Inc.
Ye, Z., Zhu, J., Li, Q., Mo, B., Lei, B., Li, Y., Wang, C., Huang, C., 2018. A novel method of reliability-centered process optimization for additive manufacturing. Microelectron. Reliab. 88–90, 1151–1156.
Yoon, H.-S., Lee, J.-Y., Kim, H.-S., Kim, M.-S., Kim, E.-S., Shin, Y.-J., Chu, W.-S., Ahn, S.-H., 2014. A comparison of energy consumption in bulk forming, subtractive, and additive processes: review and case study. Int. J. Precis. Eng. Manuf. Green Technol. 1, 261–279.
Yosofi, M., Kerbrat, O., Mognol, P., 2019. Additive manufacturing processes from an environmental point of view: a new methodology for combining technical, economic, and environmental predictive models. Int. J. Adv. Manuf. Technol. 102, 4073–4085.
Yusup, N., Zain, A.M., Hashim, S.Z.M., 2012. Overview of PSO for optimizing process parameters of machining. Procedia Eng. 29, 914–923.
Zhang, H., Nagel, J.K., Al-Qas, A., Gibbons, E., Lee, J.J.-Y., 2018a. Additive manufacturing with bioinspired sustainable product design: a conceptual model. Procedia Manuf. 26, 880–891.
Zhang, H., Xie, J., Ge, J., Lu, W., Zong, B., 2018b. An Entropy-based PSO for DAR task scheduling problem. Appl. Soft Comput. 73, 862–873.
Zhang, Y., Bernard, A., Gupta, R.K., Harik, R., 2014. Evaluating the design for additive manufacturing: a process planning perspective. Procedia CIRP 21, 144–150.
Zou, J., Chang, Q., Ou, X., Arinez, J., Xiao, G., 2019. Resilient adaptive control based on renewal particle swarm optimization to improve production system energy efficiency. J. Manuf. Syst. 50, 135–145.